4122 *Chem. Mater.* **2009,** *21,* 4122–4126
DOI:10.1021/cm8024236

CHEMISTRY OF MATERIALS
Article

Hollow Silica Spheres with a Novel Mesoporous Shell Perforated Vertically by Hexagonally Arrayed Cylindrical Nanochannels

Anfeng Zhang, Yongchun Zhang, Na Xing, Keke Hou, and Xinwen Guo*

State Key Laboratory of Fine Chemicals, School of Chemical Engineering, Dalian University of Technology, Dalian 116012, P. R. China

Received September 6, 2008. Revised Manuscript Received July 8, 2009

Hollow silica spheres with a mesoporous shell perforated by hexagonally arrayed cylindrical nanochannels have been synthesized using one-pot sol−gel/emulsion approach. Transmission electron microscopy (TEM) and scanning electron microscopy (SEM) investigations reveal that the shells of the as-made hollow silica spheres are partially covered by amorphous silica particles, which can be eliminated to a great extent after an additional hydrothermal treatment in autoclave. The hollow core structure is most likely formed by the stable benzene-in-water emulsion which acts as the removable template. And surfactant P123 favors the assembly of silica to form the mesostructured shell under acidic conditions. Using these hollow silica spheres as the hard template, structurally stable hollow carbon can be obtained, indicating that the pores on the silica shell are interconnected.

1. Introduction

Mesoporous materials with hierarchical core shell structures and well-defined morphologies have attracted much attention due to many interesting application areas.[1−6] Among many types of mesoporous materials, hollow spheres are of significance because of their potential uses in drug-delivery, adsorption, and catalysis.[7−9] Up to date, hollow spheres with various shell structures and diameters have been synthesized by different approaches. Caruso[10] and Bourlinos et al.[11] prepared hollow silica spheres via layer-by-layer self-assembly of preformed nanoparticles onto polystyrene beads or silica spheres, which are used as the templates. However, this procedure involving several deposition and washing steps is time-consuming. Moreover, the resultant shell structures are mainly as lamellar phase. A much easy approach to synthesize intact inorganic shells is the soft templating approach using vesicles and emulsion droplets as the templates.[12,13] Schacht et al.[14] first synthesized hollow silica spheres with mesopores mainly orienting radially in the shell by interfacial reactions conducted in oil/water emulsions. Lin et al.[15] extended this emulsion approach to prepare hollow spheres with the shells consisting of mesopores arranging in the latitudinal direction. Liu et al.[16] synthesized hollow spheres with the shells having randomly distributed nanochannels. Tanev and Pinnavaia[17] condensed silica in the interlayer regions of multilamellar vesicles to form nearly spherical particles with stable lamellar mesostructures. In addition, a spray drying technique is also an alternative to prepare various hollow, spherical, or collapsed, irregular particles.[18,19] Although various hollow silica spheres have been synthesized, there are, to our knowledge, no reports on the fabrication of hollow spheres with cylindrical mesopores perforating the shell.

In this paper, we report a one-pot sol−gel/emulsion approach for the synthesis of hollow silica spheres whose shells are vertically perforated by cylindrical nanochannels in the radial direction. The nanochannels with the size up to ∼11 nm are packed in a hexagonally arrayed fashion. The hollow silica spheres are structurally stable even after calcination at 540 °C for

(1) Karkamkar, A. J.; Kim, S.; Mahanti, S. D.; Pinnavaia, T. J. *Adv. Func. Mater.* **2004**, *14*, 507.
(2) Lin, H. P.; Cheng, Y. R.; Mou, C. Y. *Chem. Mater.* **1998**, *10*, 3772.
(3) Yang, M.; Ma, J.; Zhang, C.; Yang, Z.; Lu, Y. *Angew. Chem., Int. Ed.* **2005**, *44*, 6727.
(4) Khalil, A. S. G.; Konjhodzic, D.; Marlow, F. *Adv. Mater.* **2006**, *18*, 1055.
(5) Wang, B.; Chi, C.; Shan, W.; Zhang, Y. H.; Ren, N.; Yang, W. L.; Tang, Y. *Angew. Chem., Int. Ed.* **2006**, *45*, 2088.
(6) Sun, Q.; Magusin, P. C. M. M.; Mezari, B.; Panine, P.; Van Santen, R. A.; Sommerdijk, N. A. J. M. *J. Mater. Chem.* **2005**, *15*, 256.
(7) Botterhuis, N. E.; Sun, Q. Y.; Magusin, P. C. M. M.; Van Santen, R. A.; Sommerdijk, N. A. J. M. *Chem.—Eur. J.* **2006**, *12*, 1448.
(8) Zhu, Y. F.; Shi, J. L.; Shen, W. H.; Dong, X. P.; Feng, J. W.; Ruan, M. L.; Li, Y. S. *Angew. Chem., Int. Ed.* **2005**, *44*, 5083.
(9) Huang, H. Y.; Remsen, E. E.; Kowalewski, T.; Wooley, K. L. *J. Am. Chem. Soc.* **1999**, *121*, 3805.
(10) Caruso, F.; Shi, X.; Caruso, R. A.; Susha, A. *Adv. Mater.* **2001**, *13*, 740.
(11) Bourlinos, B.; Karakassides, M. A.; Petridis, D. *Chem. Commun.* **2001**, 1518.
(12) Huang, J.; Xie, Y.; Li, B.; Liu, Y.; Qian, Y.; Zhang, S. *Adv. Mater.* **2000**, *12*, 808.
(13) Imhot, A.; Ping, D. J. *Nature* **1997**, *389*, 948.
(14) Schacht, S.; Huo, Q.; Voigt-Martin, I, G.; Stucky, G, D.; Schüth, F. *Science* **1996**, *273*, 768.
(15) Lin, H. P.; Mou, C. Y.; Liu, S. B.; Tang, C. Y. *Chem. Commun.* **2001**, 1970.
(16) Liu, J.; Li, C. M.; Yang, Q. H.; Yang, J.; Li, C. *Langmuir* **2007**, *23*, 7255.
(17) Tanev, P. T.; Pinnavaia, T. J. *Science* **1996**, *271*, 1267.
(18) Bruinsma, P. J.; Kim, A. Y.; Liu, J.; Baskaran, S. *Chem. Mater.* **1997**, *9*, 2507.
(19) Lu, Y.; Fan, H.; Stump, A.; Ward, T. L.; Reiker, T.; Brinker, C. J. *Nature* **1999**, *398*, 223.

Published on Web 08/20/2009

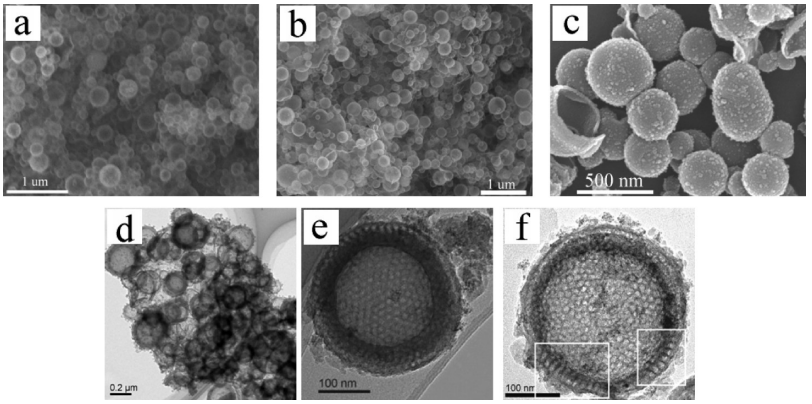

Figure 1. SEM and TEM images of the mesoporous hollow silica spheres: (a) before calcination; (b−f) after calcination.

6 h. The obtained spheres show very high specific surface area up to 700 m^2 g^{-1}, which can be potentially used as capsules for controlled release of drugs, dyes, cosmetics, and inks.

2. Experimental Section

Chemicals. All materials were of analytical grade and were used as received without any further purification. Triblock copolymer $(EO)_{20}(PO)_{70}(EO)_{20}$ (P123) was purchased from Sigma-Aldrich. Tetraethoxysilane (TEOS), acetic acid, ethanol, benzene, and other reagents were obtained from Shanghai Chemical Reagent Inc. of the Chinese Medicine Group.

Synthesis of Hollow Silica Spheres. In a typical synthesis, the molar composition of the mixture is 1.0 TEOS:0.019 P123:0.30 benzene:6.56 HCl:187.9 H_2O. Briefly, 2.0 g of P123($(EO)_{20}$−$(PO)_{70}$−$(EO)_{20}$) was first dissolved in 62.0 mL of deionized water in a sealed conical flask (100 mL) at 38 °C, followed by adding 10.0 mL of 12.0 M HCl and stirred for 1 h with a stirring rate of 800 r min^{-1}. Subsequently, 0.4 g of benzene was added to the above solution to form an emulsion under stirring. After 20 min, 4.1 mL of TEOS was added and kept on stirring for another 24 h at 38 °C. The obtained milky mixture was transferred into an autoclave and aged at 80 °C overnight under static condition. Afterward, the solid product was recovered by filtration.

Hydrothermal Treatment. To eliminate the amorphous silica particles on the surface of the hollow silica spheres, an additional hydrothermal treatment for the obtained sample was conducted in an autoclave with 50 mL H_2O at 100 °C for 4 and 12 h, respectively. Finally, hollow silica spheres with mesopores perforating the shell were obtained after filtration, washing with deioned water, drying at 60 °C, and calcination at 540 °C for 6 h.

Synthesis of Hollow Carbon Replica Spheres. The synthesis of hollow carbon replica spheres was performed by the nanocasting approach.[20,21] In brief, furfuryl alcohol was used as a carbon precursor, and oxalic acid was used as a polymerization catalyst. The furfuryl alcohol containing oxalic acid was infiltrated in hollow silica spheres by incipient wetness impregnation at room temperature, followed by polymerization at 60 °C and then 80 °C each for 16 h under air. Afterward, the composite was treated at 150 °C for 3 h, then heated to 800 °C with a heating rate of 5 °C/min and maintained at that temperature for 2 h. The carbonization procedure was performed under nitrogen flow. The obtained black powders were leached with NaOH (1 M) aqueous solution to remove the silica, further recovered by filtration, washed with distilled water and acetone, and dried at 90 °C to produce the carbon replica hollow spheres.

Characterization. Powder X-ray diffraction (XRD) patterns were recorded using a Rigaku D/Max 2400 diffractometer, which employed Cu Kα radiation. Transmission electron microscopy (TEM) images were taken on Tecnai G^2 20 S-twin instrument (FEI Company) with an acceleration voltage of 200 kV. The samples for TEM analysis were prepared by dipping the carbon-coated copper grids into the ethanol solutions of silica and drying at ambient condition. Scanning electron microscopy (SEM) images were recorded using a Hitachi S-4800. Nitrogen sorption isotherms were measured on a Micromeritics ASAP2000 sorption analyzer at liquid nitrogen temperature. Prior to the measurements, the samples were degassed at a temperature of 250 °C for overnight. Their specific surface areas were determined by the Brunauer−Emmett−Teller (BET) method, which were calculated from the adsorption data in the relative pressure intervals from 0.04−0.2. Pore size distribution curves were calculated by the Barrett−Joyner−Halenda (BJH) method from the adsorption and desorption branch, respectively. The total pore volume was estimated from the amount adsorbed at the relative pressure of 0.99.

3. Results and Discussion

3.1. As-Prepared Hollow Silica Spheres. The overall morphologies of the as-prepared samples were characterized by SEM measurements. As can be seen in Figure 1a, this sample consists of intact spheres with the sizes of several hundred nanometers. After calcination at 540 °C for 6 h, most of the spheres are still intact (Figure 1b). Some aggregated spheres are visible, which may be the result of drying and calcination processes. Figure 1c clearly shows that the spheres with the sizes from 200 to 400 nm in diameter are partially covered with some small silica particles. From the broken parts of the spheres, one can see these spheres are indeed hollow in nature. By comparing the silica spheres before (Figure 1a) and after calcinations (Figure 1b), no obvious shrinkage was observed, indicating these spheres are structurally stable.

The TEM image of the calcined samples (Figure 1d) reveals the hollow spherical morphology as well. The shell thicknesses are in the range of 40−60 nm. Clearly, hexagonally arrayed mesopores are observed throughout the shell of the hollow spheres (Figure 1e). This well-aligned

(20) Lu, A. H.; Schüth, F. *Adv. Mater.* **2006**, *18*, 1793.
(21) Lu, A.-H.; Li, W.; Schmidt, W.; Kiefer, W.; Schüth, F. *Carbon* **2004**, *42*, 2939.

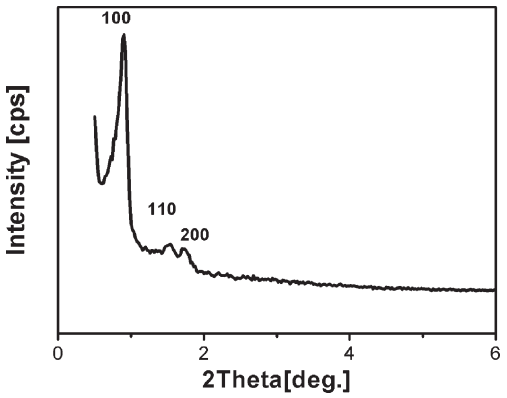

Figure 2. Low-angle X-ray diffraction pattern of calcined hollow silica spheres.

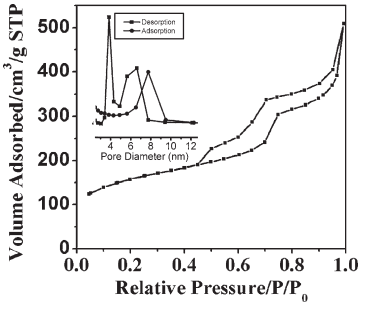

Figure 3. N_2 sorption isotherm of the calcined hollow spheres. The inset is the pore size distribution determined by the BJH method based on the desorption and adsorption branch, respectively.

structure was further verified by the XRD measurement. As shown in Figure 2, the XRD pattern of the calcined hollow silica spheres exhibits three well-resolved peaks which can be indexed as the (100), (110), (200) diffractions associated with a 2D hexagonal symmetry (*p6mm*), indicating a well-ordered mesostructure similar to SBA-15.[22] As seen in Figure 1f, the nanochannels of the hollow silica spheres perforate the shell vertically along the radial direction, which are about 40 nm in length. That is very much different from the MCM-41 type hollow spheres, of which the nanochannels orientate in the latitudinal direction.[15]

The porous nature of the hollow silica spheres are revealed by nitrogen sorption measurement. The specific surface area and pore volume are of 572 $m^2\ g^{-1}$ and 0.86 $cm^3\ g^{-1}$, respectively. As seen in Figure 3, the N_2 sorption isotherms of the hollow silica spheres is of type IV, which clearly displays two steps of capillary condensation in the range of $p/p_0 = 0.6-0.75$ and $p/p_0 = 0.75-1.0$ and does not reach a plateau. The first step corresponds to the capillary condensation of the small mesopores.[23] The second step might be related to multilayer adsorption in the larger mesopores formed between the hollow silica spheres or even the inner space of the hollow silica spheres. In desorption branch, the tail below $p/p_0 = 0.6$ indicates the existence of the partially blocked mesopores. That may be attributed to the amorphous silica coating on the shells, resulting in the partially blocked pore entrance.[23] As a consequence, the pore size distribution (PSD) curve calculated from the desorption branch exhibits a bimodal pore distribution. It should be pointed out that the pore size around 4 nm calculated from the desorption branch is not the true reflection of the PSD of this sample, that is due to instability of the meniscus at the relative pressure around 0.42.[24] In this case, the PSD calculated from the adsorption branch is provided as Supporting Information. As seen in Figure 3 (inset), the mesopore sizes of the calcined sample are mainly concentrated at 7.7 nm (adsorption branch), which is larger than that of SBA-15 synthesized at the same conditions without benzene.[25] It suggests that part of benzene may act as swelling agent to enlarge the mesopores of the shell.

3.2. Removal of Amorphous Silica Particles by Hydrothermal Treatment. As shown from the above-mentioned study, the as-prepared hollow silica spheres usually contain a small proportion of amorphous silica presenting on their external surface. That leads to a partial pore blocking effect, as revealed by the nitrogen sorption analysis. To ensure that the mesopores are open and easily accessible, to eliminate these amorphous silica particles to a great extent is more desirable. Inspired this idea, we found out that an additional hydrothermal treatment is applicable to remove the externally deposited amorphous silica particles, because at high hydrothermal temperature silica species can be slightly dissolved by water. Indeed, as seen in Figure 4a, the amorphous silica particles on the hollow silica spheres are removed from their external surfaces after the hydrothermal treatment for 4 h. That is a clear difference as compared to that in Figure 1d. Furthermore, a high magnification image displayed in Figure 4b shows the hollow silica sphere is almost free of amorphous particles on its external surface, indicating nearly complete removal of amorphous silica particles by the additional hydrothermal treatment. It is noteworthy that the cylindrical mesopores in the shells are enlarged to ~11 nm in diameter after the hydrothermal treatment (Figure 4c), that is partially due to the expansion of the micelles under a hydrothermal condition. The elimination of the amorphous silica on the surface of the hollow silica spheres are also confirmed by SEM analyses. Compared to the previous sample shown in Figure 1c, the current sample shown in Figure 4f has much less amorphous silica particles covered on the external surfaces of the hollow silica spheres. Thus, we can conclude that hydrothermal treatment can, to a great extent, eliminate the amorphous silica attached on the hollow spheres.

The N_2 sorption isotherm of the calcined hollow silica spheres after hydrothermal treatment for 4 h (Figure 5a) are still of type IV and display a large hysteresis loop,

(22) Zhao, D. Y.; Feng, J. L.; Huo, Q. S.; Melosh, N.; Fredrickson, G. H.; Chmelka, B. F.; Stucky, G. D. *Science* **1998**, *279*, 548.
(23) Voort, P. V. D.; Ravikovitch, P. I.; de. Jong., K. P.; Neimark, A. V.; Janssen, A. H.; Benjelloun, M.; Bavel, E. V.; Cool, P.; Weckhuysen, B. M.; Vansant, E. F. *Chem. Commun.* **2002**, 1010.
(24) Thommes, M.; Köhn, R.; Fröba, M. *Appl. Surf. Sci.* **2002**, *196*, 239.
(25) Zhao, D. Y.; Huo, Q. S.; Feng, J. L.; Chmelka, B. F.; Stucky, G. D. *J. Am. Chem. Soc.* **1998**, *120*, 6024.

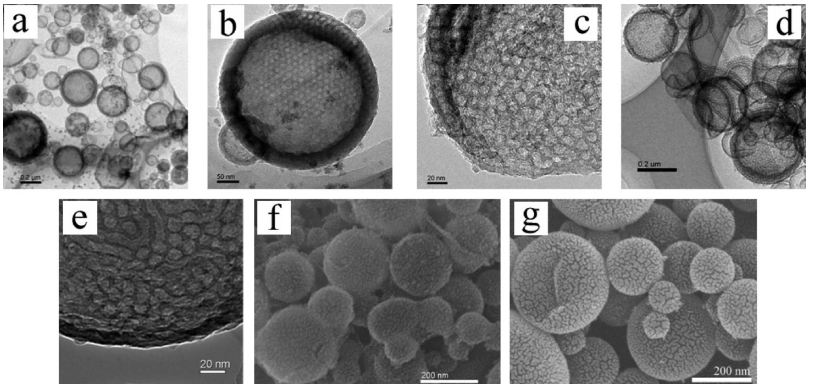

Figure 4. TEM and SEM images of the mesoporous hollow silica spheres after hydrothermal treatment: (a, b, c, f) for 4 h; (d, e, g) for 12 h.

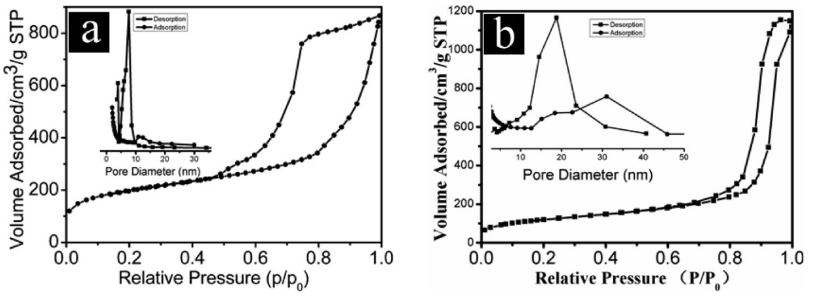

Figure 5. N_2 sorption isotherm of hollow spheres after hydrothermal treatment calcined: (a) for 4 h; (b) for 12 h. The inset is the pore size distribution determined by the BJH method based on the desorption and adsorption branch, respectively.

indicating the presence of mesopores.[26] Moreover, the isotherm did not reach a plateau at the relative pressure close to 1, which indicates the existence of larger mesopores and/or macropores, probably corresponding to the continuous condensation of nitrogen molecules within the large caves of ~200 nm (or even smaller) of the hollow silica spheres. Considering the TEM images shown in Figure 1f and 4b, it is reasonable to say that the inner space of the hollow spheres after hydrothermal treatment is accessible. Compared with the N_2isotherm of the calcined hollow silica spheres without hydrothermal treatment, the tail in the desorption branch becomes much smaller, indicating the pore blocking effect due to the existing of the amorphous silica particles is minimized. As calculated from the adsorption branch, the mesopore sizes of the hollow silica spheres are about 10.7 nm, which is in line with the data obtained from TEM (Figure 4c) and larger than that of the samples without hydrothermal treatment. Furthermore, the specific surface area and pore volume were 706 $m^2\ g^{-1}$ and 1.34 $cm^3\ g^{-1}$, respectively. These values are much greater than those of the hollow silica spheres without hydrothermal treatment. The increased surface area and pore volume is attributed to the removal of amorphous silica particles (species) in the silica shell and within the mesopores, leading to pore opening.

Notably, longer hydrothermal treatment leads to nearly complete remove of amorphous silica particles. For example, when the sample is treated in an autoclave at 100 °C for 12 h, the tail below $p/p_0 = 0.6$ in the desorption branch disappears completely (Figure 5b), indicating the pore opening effect by eliminating the amorphous silica particles on the shell, which also can be confirmed by the SEM analyses (Figure 4g). Compared to the hollow silica spheres shown in Figure 4f, the spheres in Figure 4g are almost free of amorphous species on their external surface. Meanwhile, the shells of the hollow silica spheres are getting thinner and even distorted (Figure 4d). Clearly, longer hydrothermal treatment also results in the dissolution of the silica species within the mesopores. Some micropores connecting the mesopores were enlarged to mesopores, and some mesopores are united into larger ones of ~30 nm (Figure 4e and 5b), which leads to the decreasing of surface area to 433 $m^2\ g^{-1}$ and the increasing of pore volume to 1.78 $cm^3\ g^{-1}$, respectively. The arrangement of the mesopores also becomes irregular (Figure 4c−e), which can be confirmed by the XRD analysis, i.e., no well-resolved peaks in the XRD pattern (not shown here) of the samples after hydrothermal treatment were observed.

By combining the results from N_2 sorption and TEM analyses, one can conclude that the hydrothermal treatment enlarges the mesopores in the shell by micelles expansion as well as elimination of silica particles (species) on the shell and within the mesopores.

3.3. Carbon Replica from the Hollow Silica Spheres. The characterization results from TEM, XRD, and nitrogen sorption clearly show that the mesostructure of the hollow silica spheres is similar to that of SBA-15. Many studies have demonstrated that mesoporous silica is a suitable hard template for the synthesis of ordered mesoporous carbons, due to its well-developed

(26) Ravikovitch, P. I.; Neimark, A. V. *Langmuir* **2002**, *18*, 1550.

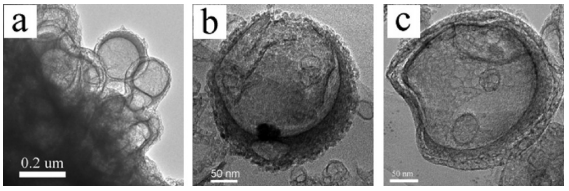

Figure 6. TEM images of the carbon replica from the hollow silica spheres.

pore interconnectivity.[27,28] Hence, in this study, hollow carbon replica spheres were prepared using calcined hollow silica spheres, which have been treated by additional hydrothermal aging for 4 h, as the templates via nanocasting approach, thus to investigate the pore interconnectivity of the hollow silica spheres. The carbon precursor was introduced into the pores of silica template by incipient wetness impregnation. As shown in Figure 6, the TEM images display that hollow carbon spheres can be obtained by the nanocasting approach. Due to the variety of the size and the thickness of the hollow silica sphere templates, the size and the thickness of the carbon replica exhibit large variety as well. In this study, the preparation of uniform carbon replica spheres is not our objective. Instead, we are interested in the interconnectivity of the silica structure. The mesopores in the nanocast carbon shell are visible. The obtained carbon hollow spheres demonstrate that the hollow silica spheres can be used as hard templates, and the mesopores in the silica shells are well-interconnected.[27,28] Hence, this experiment reveals that the mesostructure of the hollow silica spheres are stable during the calcination and nanocasting steps.

On the basis of the above-mentioned results, we presumably propose that the formation of hollow silica spheres essentially involves a self-assembly of silica around the soft template, that is similar to the formation mechanism of SBA-15.[29,30] However, there is a clear difference between these two kinds of silica products. Apparently, the presence of a benzene/water emulsion is the crucial factor for the formation of hollow silica spheres.[14] In the benzene/water system, P123 molecules concentrate at the benzene/water interface as emulsifier to stabilize the benzene-in-water emulsion droplets,[31,32] then silicate species and P123 micelles self-assemble into a 2-dimensional (2D) hexagonal arrangement on the surface of the droplets of benzene. The perforated shell with hexagonally arrayed cylindrical nanochannels of ~40 nm in length along the radial direction suggests that the mesoporous structure of the shell is most likely formed along the short axis[33] rather than along the periphery forming the layered structure.[34] Since the working window of this kind of hollow silica spheres is quite narrow, an optimized synthetic condition including the molar ration of P123/benzene, the pH (influencing the hydrolysis and assembly process of TEOS), and the reaction temperature guarantees successful preparation of hollow silica spheres with the specially orientated nanochannels.

4. Conclusion

We have demonstrated that the hollow silica spheres with hexagonally arrayed cylindrical nanochannels along the radial direction were synthesized using a one-pot sol−gel/emulsion technique. Importantly, an additional hydrothermal treatment is a necessary step to smooth the external surface of the hollow silica spheres by eliminating the attached amorphous silica particles, which also results in the opening of the partially blocked mesopores. These hollow silica spheres are structurally stable and have well-interconnected mesopores in the shells, as revealed by their carbon replica obtained by the nanocasting approach. Owing to the special arrangement of the mesopores, i.e., hexagonally arrayed mesoporous structure along the radial direction, the hollow silica spheres are potentially useful in applications such as encapsulation, delivery, controlled-release applications.

Acknowledgment. This project was sponsored by Program for New Century Excellent Talents in University (NCET-04-0268) and by the 111 Project. The author thanks Prof. Roel Prins and Prof. Wencui Li for their thoughtful discussion.

(27) Ryoo, R.; Joo, S. H.; Jun, S. *J. Phys. Chem. B* **1999**, *103*, 7743.
(28) Arnal, P. M.; Schüth, F.; Kleitz, F. *Chem. Commun.* **2006**, 1203.
(29) Flodström, K.; Wennerström, H.; Alfredsson, V. *Langmuir* **2004**, *20*, 680.
(30) Ruthstein, S.; Schmidt, J.; Kesselman, E.; Talmon, Y.; Goldfarb, D. *J. Am. Chem. Soc.* **2006**, *128*, 3366.
(31) Langevin, D. *Acc. Chem. Res.* **1988**, *21*, 255.
(32) Kabalnov, A.; Lindman, B.; Olsson, U.; Olsson, L.; Thuresson, K.; Wennerström, H. *Colloid Polym. Sci.* **1996**, *274*, 297.
(33) Zhang, H.; Sun, J. M.; Ma, D.; Bao, X. H.; Hoffmann, A. K.; Weinberg, G.; Su, D. S.; Schlögl, R. *J. Am. Chem. Soc.* **2004**, *126*, 7440.
(34) Sun, Q. Y.; Kooyman, P. J.; Grossmann, J. G.; Bomans, P. H. H.; Frederik, P. M.; Magusin, P. C. M. M.; Beelen, T. P. M.; Van Santen, R. A.; Sommerdijk, N. A. J. M. *Adv. Mater.* **2003**, *15*, 1097.